ELSEVIER

Biophysical Chemistry 110 (2004) 281–295

Biophysical Chemistry

www.elsevier.com/locate/bpc

Aggregation properties of a HPMA-camptothecin copolymer in isotonic solutions

Giuseppe Chirico[a,*], Maddalena Collini[a], Francesca Olivini[a], Moreno Zamai[b], Enrico Frigerio[c], Valeria R. Caiolfa[d]

[a] *Department of Physics, Università di Milano-Bicocca, and Istituto Nazionale per la Fisica della Materia, Piazza della Scienza 3, 20126 Milan, Italy*

[b] *Discovery Research Oncology, Pharmacia Corporation, V.le Pasteur 10, 20014 Nerviano, Milan, Italy*

[c] *Global Drug Metabolism Research, Pharmacia Corporation, V.le Pasteur 10, 20014 Nerviano, Milan, Italy*

[d] *Fondazione Centro San Raffaele, Scientific Institute, Via Olgettina 58, 4 A1, 20132 Milan, Italy*

Received 24 January 2004; received in revised form 2 March 2004; accepted 5 March 2004
Available online 5 May 2004

Abstract

Copolymers of camptothecin (CPT) and [*N*-(2-hydroxypropyl) methacrylamide] (HPMA) are novel anticancer drugs that show improved pharmacological profile in animal models as compared to the free drug CPT. We investigate here the aggregation properties of a HPMA-glycyl-6-aminohexanoyl-glycyl-CPT copolymer (~ 20,000 Da). The molecular size of HPMA-copolymer CPT is followed over 5 orders of magnitudes of concentration in isotonic buffer by measuring either the time resolved fluorescence anisotropy (FA) of CPT or the autocorrelation function of the light scattered by the copolymer. A detailed analysis of these data suggests the presence of elongated structures with axial ratio ~ 3 in the range 0.1–0.5 μg/ml and aggregates with association number higher than 2 in more concentrated solutions (up to 10 mg/ml). The binding affinity of HPMA-copolymer CPT for serum albumin is inversely dependent on the degree of aggregation of the copolymer. We also show that the copolymer concentration in plasma from mice treated with an active, non-toxic, dose of HPMA-copolymer CPT, decreases from 3 to 0.01 mg/ml in 72 h. In the same range of concentrations in vitro, we do not detect hydrophobic aggregates of polymers with high (>3) association number. Our study indicates that the circulating HPMA-copolymer CPT in mice should not undergo extensive aggregation and should interact with serum albumin more weakly than free CPT.

Keywords: HPMA; Fluorescence anisotropy; Photon correlation spectroscopy; Aggregation; Camptothecin; Drug delivery

1. Introduction

Development of efficient drug delivery systems and its understanding on a physical and chemical grounds has attracted tremendous attention during the last two decades [1,2]. Researchers have soon realized the enormous barriers that a drug molecule must overcome before it reaches its target site within the body [3] and have envisioned the possibility, by means of specific drug delivery systems, to address and correct problems related to the physical characteristic of simple drugs, including solubility, stability and, most of all, toxicity.

* Corresponding author. Tel.: +39-2-64482872; fax: +39-2-64482894.
E-mail address: giuseppe.chirico@unimib.it (G. Chirico).

0301-4622/$ - see front matter © 2004 Elsevier B.V. All rights reserved.
doi:10.1016/j.bpc.2004.03.004

The use of polymeric drug carriers is an established approach for improvement of cancer chemotherapy [4,5]. The covalent binding of low molecular weight drugs to water-soluble polymer carriers offers a potential mechanism to enhance the specificity of drug action. Specificity might be achieved either by an active targeting of polymer-drug conjugates to cancer cells or passive accumulation of conjugates within solid tumors [4,5].

This has led to the emergence of a new field called 'polymer therapeutics' [2] in which the physical characterization of these polymeric systems and of their interactions with the major plasma components plays a central role.

We study here the aggregation properties in isotonic buffer of a [*N*-(2-hydroxypropyl) methacrylamide] (HPMA)-copolymer of the antineoplastic drug camptothecin (CPT), which showed an impressive antitumor activity in animal models [6–8] and it is at present under clinical evaluation [9,10]. The antitumor efficacy of CPT was established in experimental models [6,7] in the early 1960s. In the 1970s, due to the limited CPT solubility in water, a water-soluble sodium salt of the drug (carboxylate form) was formulated for use in clinical trials, but showed significant toxicity [9,11,12]. During the next 20 years, the discovery of topoisomerase I as the cellular target of camptothecin and its analogues [13–15] renewed the interest on this class of compounds, since topoisomerase I is expressed in advanced stages of human colon adenocarcinoma and other malignancies but not in normal tissue [16,17]. Structure–activity relationship studies on semi-synthetic and synthetic camptothecin derivatives [18] highlighted the importance of the lactone, closed ring molecule for drug activity and, in retrospect, recognized that the carboxylate form of CPT results in insufficient amounts of the active form being available.

The synthesis and the antitumor activity of HPMA-copolymers of CPT was previously described [8,19]. In

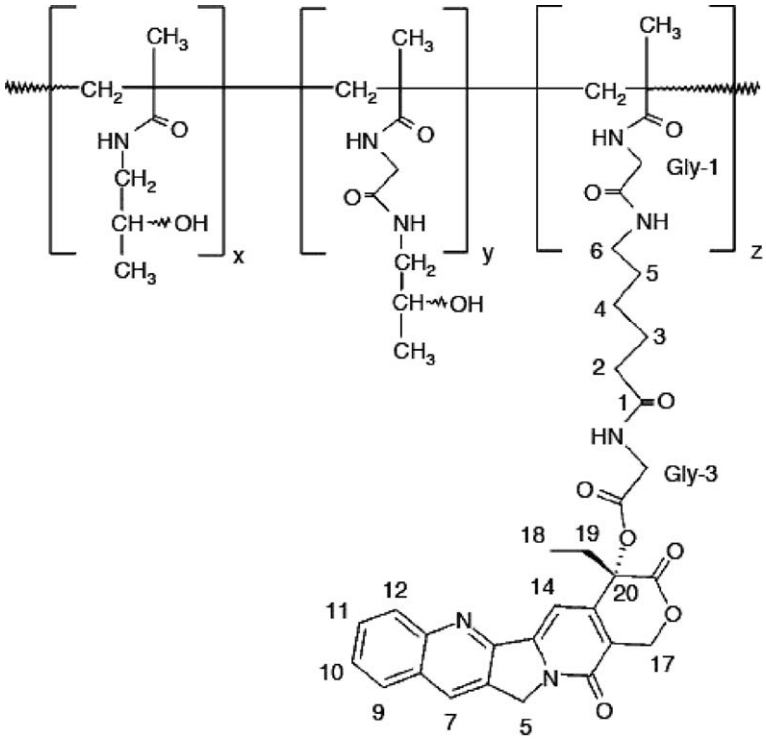

Scheme 1. HPMA-copolymer CPT: structure. The chemical characteristics of HPMA-copolymer CPT were: biodegradable side chain-glycyl-6-aminohexanoyl-glycyl; CPT content 9.1% (w/w); M_n (weight-average molecular weight) 19,300 Da; M_w/M_n (polydispersity) 1.07; free intermediate (side chain-CPT) <0.005% (w/w); extinction coefficient (cm^{-1} M^{-1}) ε_{364}=19,097.

these conjugates, the lactone form of CPT is covalently linked at its α-hydroxyl group to the polymer through a biodegradable spacer such as an oligopeptide [4,19,20] or the glycyl-6-aminohexanoyl-glycyl linker (Scheme 1). HPMA-copolymers of CPT are water-soluble macromolecules that partly protect the active lactone form of CPT in plasma and allow modulation of CPT release by esterolytic and proteolytic cleavage at the tumor site, according to the chemical features of the degradable spacer. We have showed that the therapeutic index of CPT in vivo can be remarkably enhanced when conjugated in HPMA-copolymers [8,19], due to the so called "enhanced permeability and retention" effect [21–25]. The abnormal vasculature of tumors shows an increased vessel permeability, which allows extravasation of large molecules more than in normal tissues. At the same time, the poor lymphatic drainage of tumors allows high concentrations of copolymeric drug to build up in these tissues. Careful design of the biodegradable spacer can tailor the conjugate as a prodrug for activation by various hydrolytic and proteolytic mechanisms [4,8,19]. This leads to very low levels of free drug released in the circulation and it results in a substantial decrease of systemic toxicities as compared with the free drug [4,8,19]. On the other hand, the binding of a hydrophobic moiety such as CPT to side chain termini of the hydrophilic HPMA-copolymer determines its amphiphilic properties in aqueous phase, where the copolymers may experience CPT-CPT intramolecular interaction and inter-molecular association. The formation in vivo of hydrophobic associates of HPMA-CPT copolymers, in fact, might affect the pharmacokinetic profile and modulate the accumulation in solid tumors.

In this work, we investigate the aggregation properties in isotonic buffer solutions of the HPMA-copolymer CPT in Scheme 1. In this particular conjugate, at 9.1 % w/w drug content, the drug is covalently linked at the C-20 position via the biodegradable spacer-glycyl-6-aminohexanoyl-glycyl. We use either dynamic light scattering (DLS) or time resolved fluorescence anisotropy (FA) to characterize the random association of the HPMA-copolymer CPT in a wide range of concentrations (5 orders of magnitude). We also examine in what extent aggregation modifies the interaction of the copolymer with human serum albumin (HSA), the major carrier protein in plasma. Our study lays the ground for interpreting the pharmacokinetics and toxicity of the conjugate in vivo on the basis of the aggregation and protein binding properties.

2. Experimental

2.1. Compounds

Chemicals were reagent grade or better. HSA (A1553 CAS 70024-90-7) and CPT (C9911 CAS 7689-03-4) were purchased from Sigma. HPMA copolymer of CPT was synthesized by the Pharmacia (Scheme 1). The degradable spacer-glycyl-6-aminohexanoyl-glycyl (–Gly–C_6–Gly–) was introduced for conjugating HPMA to the α-hydroxyl group of CPT, according to a previously described three-step procedure [19], which yields conjugates free of contaminants (side chain-CPT) <0.005%. The product (weight-average molecular weight of 20,400 Da and polydispersity, M_w/M_n, of=1.45) was then fractionated by size exclusion chromatography. The fraction with M_n=19,300 Da (13,000<90% M_w> 30,000), polydispersity 1.07, drug content 9.1% (w/w), was used for this study. Weight-average (M_w) and polydispersity (M_w/M_n) were determined by size exclusion chromatography [26] in non-polar solvents. Drug content was quantified by total hydrolysis [19].

2.2. Sample preparation

Stock solutions of HPMA-copolymer CPT were prepared in DMSO to avoid spontaneous hydrolysis during storage. Immediately before in vitro experiments, the conjugate was diluted in phosphate-buffered saline (PBS, 160 mM) pH 7.4 previously filtered with a 0.22-μm Millipore Durapore membrane. The residual DMSO content was always less than 0.05%. HPMA-copolymer CPT concentrations, checked photometrically by employing ε_{364}=19,097 M^{-1} cm^{-1}, were expressed as HPMA-CPT copolymer weight/volume. HSA crystallized powder was dissolved in PBS and protein concentrations was determined photometrically by the absorbance at 280 nm (ε=28,780 M^{-1} cm^{-1} in PBS pH 7.4). All aqueous solutions were used promptly after preparation.

2.3. Fluorescence spectroscopy

Steady state fluorescence emission and excitation spectra were performed on a Varian Eclipse (Varian, Torino, I) spectrofluorometer. The time-resolved fluorescence in the frequency domain was followed by a K2 multifrequency modulation fluorometer (ISS, Urbana-Champaign, IL) with excitation provided by the 364-nm output of an argon ion laser (2025, Spectra Physics, Mountain View, CA). The radio frequency modulated laser intensity (from 0.6 to 300 MHz) was sent to a quartz 10 mm path cell, thermostated at 20±0.2 °C, and the fluorescence signal was collected at 90° through a 435-nm long pass filter. For lifetime measurements, the emission polarizer was set at the magic angle position [27], and a solution of bis-MSB (1,4-bis(2-methylstyryl)benzene) in cyclohexane was used as the reference sample of known lifetime [28], τ=1.49 ns. The phase shift and the demodulation of the fluorescence signal with respect to the incident signal were acquired versus the modulation frequency. In general, the fluorescence lifetime decay can be analyzed as a sum of N exponential components:

$$I(t) = \sum_{i=1...N} \alpha_i \exp[-t/\tau_i] \tag{1}$$

where α_i are the pre-exponential factors and τ_i are the corresponding lifetime values. Data fitting involves a Laplace transform of the fluorescence intensity [27,29]. It yields lifetime values τ_i and fractional intensities f_i:

$$f_i = \frac{\alpha_i \tau_i}{\sum_{i=1...N} \alpha_i \tau_i} \tag{2}$$

For time-resolved FA, the sample was excited by a vertically polarized light and the emission was detected both in the parallel ($I_\parallel$) and in the perpendicular ($I_\perp$) polarizers orientations. The two components of the fluorescence intensity are related to the fluorescence anisotropy, $r(t)$, by:

$$I_\parallel(t) = \frac{I_0}{3}(1 + 2r(t)) \quad I_\perp(t) = \frac{I_0}{3}(I - r(t)) \tag{3}$$

In the frequency domain, the Laplace transform of the perpendicular and parallel components of the fluorescence intensity (Eq. (3)) are used to fit the experimental values of the phase angles difference and demodulation ratios [27,29,30].

We have always found that the anisotropy of HPMA-copolymer CPT can be fitted by the sum of just two exponentials:

$$r(t) = r_0[g_1 \exp(-t/\phi_1) + g_2 \exp(-t/\phi_2)] \tag{4}$$

where r_0 is the limiting anisotropy, and ϕ_1 and ϕ_2 are the two rotational correlation times of amplitude g_1 and g_2=1−g_1. We can obtain an estimate of the molecular size from the rotational correlation time making some hypotheses on both copolymer shape and viscosity. Solvent viscosity well approximates solution viscosity in this case, because the highest concentration in our fluorescence studies is ≅20 μg/ml and the polymer intrinsic viscosity [26] is ≅0.11 dl/g.

As far as the copolymer shape is concerned, even for a simple cylindrical symmetry the rotational diffusion is characterized by two coefficients, $D_{\text{rot}\parallel}$ and $D_{\text{rot}\perp}$, which depend on the cylinder length and axial ratio [31]. In this case, the fluorescence anisotropy decay $r(t)$ is given by the sum of three exponentials [32] with rotational correlation times (Φ_i):

$$\Phi_1 = \frac{1}{6D_{\text{rot}\perp}} \quad \Phi_2 = \frac{1}{5D_{\text{rot}\perp} + D_{\text{rot}\parallel}}$$

$$\Phi_3 = \frac{1}{4D_{\text{rot}\perp} + 2D_{\text{rot}\parallel}} \tag{5}$$

However, in some cases, the fluorescence anisotropy decay can be described by a single exponential as, for instance, when the macromolecule has a small axial ratio or when several fluorescent probes are attached to the same macromolecule. The apparent rotational correlation time is then given by the harmonic average of the three rotational correlation times over the orientation of the dipole moment:

$$1/\phi_{\text{harm}} = (1/r_0)\sum r_i/\Phi_i \tag{6}$$

where r_i are the relative weights of the three rotational correlation times given in Eq. (5). In the particular case in which the transition moments are randomly oriented with respect to the axes of the particle, one obtains [32]:

$$\phi_{\text{harm}} = 1/(0.2/\Phi_1 + 0.4/\Phi_2 + 0.4/\Phi_3) \tag{7}$$

As further discussed in Section 4, the rotational correlation times of all our experiments were well described by the latter simplified relationship.

2.4. Dynamic light scattering

For DLS, the vertically polarized laser light (wavelength=532 nm in TEM00 mode) was spatially filtered and focused in the middle of a thermostated square quartz cell with 10 mm optical path. The light scattered at 90° was detected through a multimode optical fiber, the output of which was coupled to two photomultipliers tubes (H5873P-01, Hamamatsu, Japan) through a 50% beam splitter and the auto-correlation function (ACF) was measured as a pseudo-cross-correlation function by means of an ALV5000E/fast digital correlator (ALV, Langen, D). Further details on this set-up can be found elsewhere [33]. The ACF of the vertically polarized scattered light intensity gives information mainly on the translational diffusion process [35], which depends also on the size of HPMA-CPT copolymers. In our studies, the HPMA-CPT copolymer had a polydispersity of only 1.07 and, therefore, a single exponential fit according to:

$$G^{(2)}(t) = \langle I(t)\rangle_t^2(1 + f\exp[-2\Gamma t]) \quad (8)$$

was adequate to describe the autocorrelation functions. In Eq. (8), Γ is the translational diffusion rate, f is an arbitrary fitting parameter (~ 0.4) and $\langle I(t)\rangle$ is the average scattered light. The translational diffusion coefficient, D_T, is obtained from the relaxation rate as $D_T=\Gamma/q^2$, where $q=4\pi n \sin(\theta/2)/\lambda$, n is the solution refraction index, λ is the vacuum wavelength and $\theta=90°$. The refraction index of the HPMA-CPT copolymer solutions was measured by an Abbe refractrometer (Atago 3T, Atago, Japan) finding an increase $\partial n/\partial C \cong 0.2$ cm^3/g at T=20 °C. All measurements were reported to the standard case of water at T=20 °C according to the relationship, $D_{20}=D_T(293.15/0.01)(\eta/T)$. The viscosity of the solution was obtained by considering the intrinsic viscosity, $[\eta]$=0.11 dl/g as it is obtained for HPMA-CPT copolymer of M_n=19,300 Da [26]. Accordingly, we have applied the proper correction to the translational diffusion coefficient in the full concentration range. A maximum of +20% correction was reached at 20 mg/ml. Also, we have evaluated that, without applying the second order correction (Huggins coefficient), we underestimate the translational diffusion coefficient by 2% at the most. Minor corrections on the translational diffusion coefficient due to polydispersity are discussed below (see Section 4).

Molecular shape also affects the relationship between molecular size and translational diffusion rate. The diffusion of a cylindrical molecule is characterized by two translational coefficients, $D_{T\parallel}$ and $D_{T\perp}$, along the two principal axes [36]. These coefficients depend on the cylinder length and on its axial ratio [32], and the experimental diffusion coefficient (D) has obtained from [36]:

$$D = (D_{T\parallel} + 2D_{T\perp})/3 \quad (9)$$

2.5. Plasma levels of HPMA-copolymer CPT in healthy mice

Plasma levels were determined after single intravenous injection in Balb-c male mice. HPMA-copolymer CPT was administered in sterile 0.9% NaCl solution at the dose of 220 mg/kg, which is equivalent to 20 mg/kg of CPT in this case since drug loading is 9.1% (see Section 2.1). Blood was collected from three mice per time point in heparinized tubes just before dosing (time 0) and at several times up to 72 h after administration. The assessment of HPMA-copolymer CPT concentration was carried out by chemical hydrolysis in borate buffer (pH 9.8) followed by solid-phase extraction and determination of CPT in RP-HPLC, as previously described [19].

3. Results

3.1. The fluorescence emission of CPT is reduced in the copolymer conjugate

Fig. 1 shows fluorescence excitation and emission spectra of HPMA-copolymer CPT and of the free drug, CPT, at neutral pH. Since the two spectra are obtained at the same value of absorbance, i.e., at the same excitation probability, the differences found in the emission intensity can be directly interpreted as

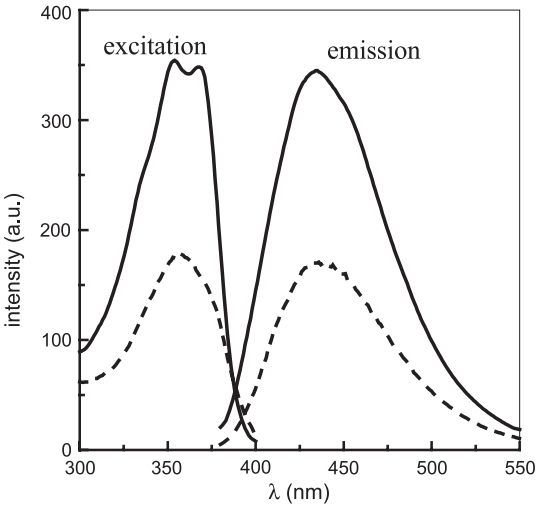

Fig. 1. Fluorescence excitation and emission spectra in arbitrary units of CPT (continuous line) and of HPMA-copolymer CPT (dashed line). The emission and excitation spectra were acquired at λ_{ex}=364 and λ_{em}=436 nm, respectively. Spectra were taken at the same value of absorbance of HPMA-copolymer CPT and CPT in isotonic buffer, pH 7.4.

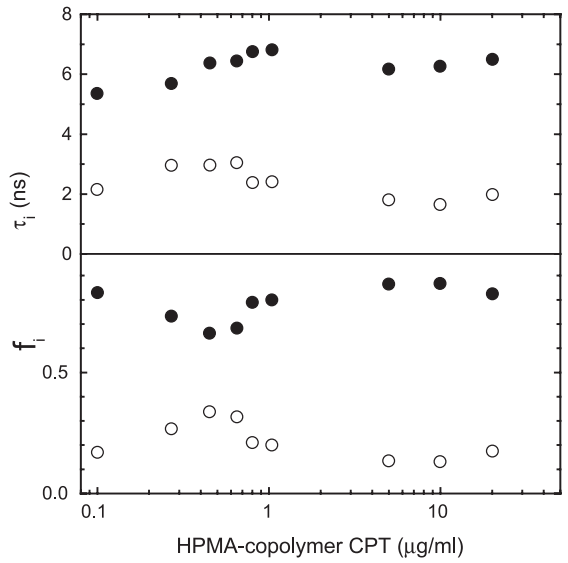

Fig. 2. Fluorescence lifetimes of CPT as a function of the copolymer concentration. Upper panel: values of τ_1 and τ_2; lower panel: fractional intensities f_1 and f_2. Full symbols refer to the long lifetime component (1) and open symbol to the short one (2). Error bars are of the same magnitude of the symbol size or less.

variations in the quantum yield of the CPT when free in solution or linked to the polymer.

3.2. In dilute solutions, an aggregation transition is detected by fluorescence lifetime and anisotropy

The aggregation of HPMA-copolymer CPT could be followed by fluorescence in the range of 100 ng/ml–20 μg/ml, before saturation effects start to occur. In this range, the fluorescence decay of HPMA-copolymer CPT in buffer at neutral pH is heterogeneous (Fig. 2). The decay is satisfactory described by two exponential components: a long lifetime, 5.3–6.8 ns, which accounts for 70–85% of the emission, and a short one, 1.8–3 ns. A Lorentzian distribution analysis does not improve the fit, therefore indicating the presence of two distinct components. In contrast, native CPT in buffer has a single fluorescence lifetime, which is 3.7 ns for the lactone (the predominant form at acidic pH) and 4.0 ns for the carboxylate form at neutral pH [8].

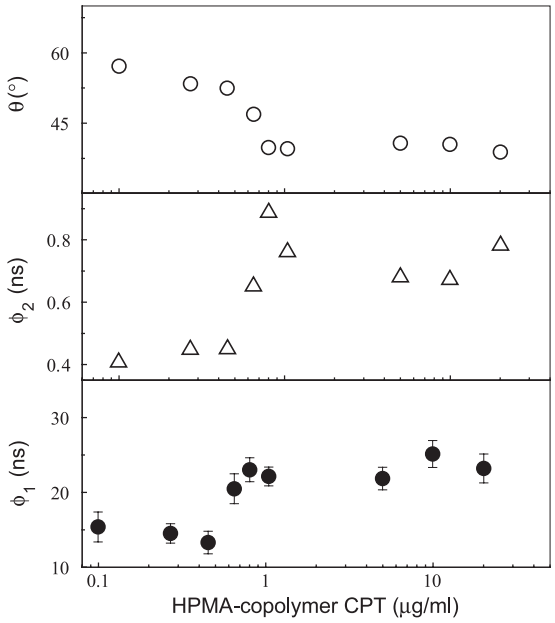

Fig. 3. Fluorescence anisotropy as a function of HPMA-copolymer CPT concentration. Lower panel: long rotational correlation time ϕ_1; central panel: short correlation time ϕ_2. Upper panel: maximum wobbling angle of CPT bound to the copolymer as derived from Eq. (12). Rotational correlation times were obtained from Eq. (4). Where not present, error bars are of the same magnitude of the symbol size or less.

The fluorescence lifetimes τ_1 and τ_2 and the fractional intensities f_1 and f_2 depend on the concentration of the fluorophore (Fig. 2). Both lifetimes show a slight change and seem to reach a constant value of 2 and 6 ns, respectively, at about 0.3–0.4 μg/ml.

Also FA data are best-fitted only by two rotational correlation times, ϕ_1 and ϕ_2, using Eq. (4). At ~0.5 μg/ml, the long rotational correlation time, ϕ_1, increases sharply from 14.4±1 to 23.0±1.3 ns (Fig. 3). In parallel, the short component, ϕ_2, raises from 0.4 to 0.7 ns, always at least one order of magnitude smaller than ϕ_1. These rotational correlation times can be reasonably identified with those obtained in cases of hindered segmental motion of a small fluorophore conjugated to a macromolecule ($\phi_2<\phi_1$) [27]. Accordingly, we can interpret the motion described by ϕ_1 as the overall rotation of HPMA-CPT copolymer, while ϕ_2 represents the hindered segmental motion of CPT.

3.3. In concentrated solutions, a continuous aggregation process is detected by dynamic light scattering

An example of the ACF of the scattered light intensity is shown in Fig. 4. The ACF, fitted [33] with Eq. (8), yields the translational diffusion coefficient, D_T (see Section 2). A constant diffusion coefficient D_{20} is found up to ~300 μg/ml and it decreases at higher concentrations. This suggests a progressive aggregation, since D_{20} is inversely proportional to the molecular radius. Repulsive interaction effects on the translational diffusion are negligible because the copolymer is not charged at pH 7.4 and the maximum volume fraction (at the highest concentration, i.e. 20 mg/ml) is ~0.02. The contribution from hard core interactions can vary only slightly [37,38], and leads either to a +3% overestimate or to a −1.8% underestimate of D_{20}. This uncertainty is within the experimental errors. Moreover, in order to ensure that no

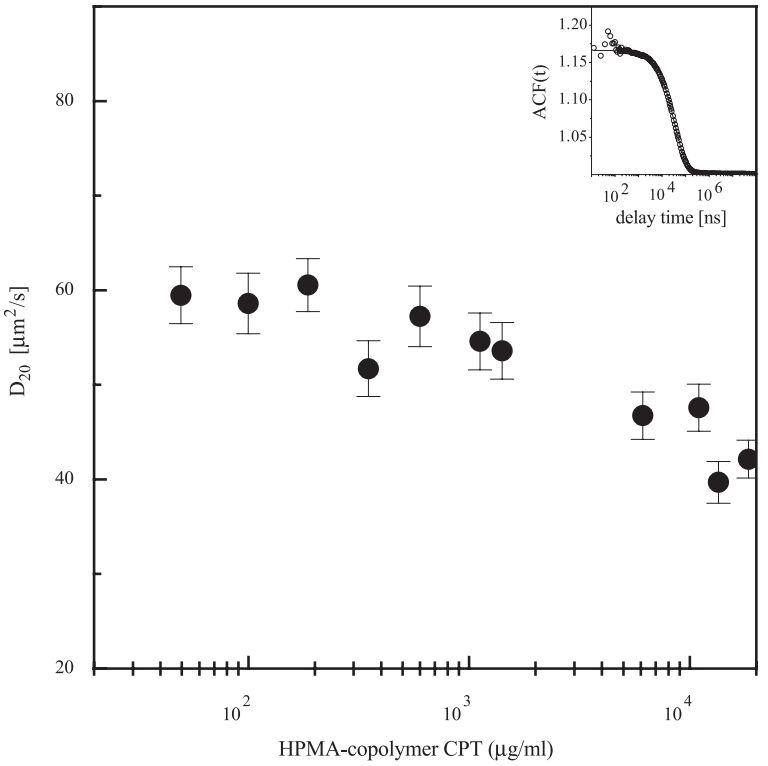

Fig. 4. Dependence of the translational diffusion coefficients, D_{20}, on HPMA-copolymer CPT concentration. Error bars: standard deviation. Inset: typical ACF (open circle) fitted by Eq. (8) (solid line).

thermal auto-absorbing effects were taking place at high copolymer concentration, we have verified that D_{20} at 11 mg/ml was independent on laser power, from 70 to 300 mW (data not shown).

3.4. Aggregation decreases the interaction of HPMA-CPT copolymer with serum albumin

We evaluate the binding of HPMA-copolymer CPT to HSA in buffer solutions at isotonic conditions and pH=7.4. HPMA-copolymer CPT is titrated with HSA and the binding measured by FA. We have repeated titration at three concentrations of HPMA-copolymer CPT: 0.34, 1.7 and 10 μg/ml. The fluorescence anisotropy of CPT in the presence of HSA still follows a double-exponential decay with the long rotational correlation time (ϕ_1) representing a weighed average of the contributions from HPMA-copolymer CPT and HPMA-copolymer CPT:HSA complex. At each HPMA-copolymer CPT concentration, ϕ_1 increases up to a plateau (Fig. 5). The shorter rotational correlation time (ϕ_2) stands for the probe segmental motion

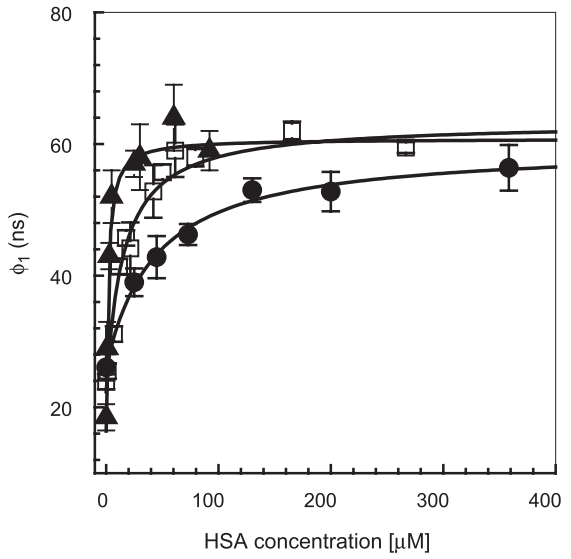

Fig. 5. Binding of HSA to HPMA-copolymer CPT in isotonic buffer, at pH 7.4 followed by the increase of the long rotational correlation time of HPMA-copolymer CPT (ϕ_1). Titration with HSA is carried out at three fixed concentrations of HPMA-copolymer CPT: 0.34 μg/ml (full triangles), 1.7 μg/ml (open squares), 10 μg/ml (full circles). The solid lines represent the best-fitted binding curves obtained from Eqs. (10) and (11). Fitting parameters are shown in Table 1.

Table 1
Binding parameters derived from HSA best-fitted titration curves at fixed HPMA-copolymer CPT concentration, assuming n=1, in comparison with the free drug, CPT

[HPMA-copolymer CPT]	ϕ_1^∞ (ns)	ϕ_1^0 (ns)	K_d (μM)	χ^2
0.34 μg/ml	60.8±1.8	16.4±1.9	1.8±0.4	0.6
1.7 μg/ml	63.0±0.8	22.4±0.9	14.7±1.6	2.8
10 μg/ml	59.7±1.4	26.0±1.0	42±6	1.3
Carboxylate CPT[a]	–		3.6±0.2	–
Lactone CPT[a]	–		6±1	–

ϕ_1^∞ is the extrapolated plateau value at saturation and ϕ_1^0 is the rotational correlation time of HPMA-copolymer CPT in the absence of HSA. K_d is the dissociation constant in μM units. χ^2 is the reduced chi-square [55].

[a] Binding of free CPT was carried out by following the fluorescence quenching of the single tryptophan residue of HSA (1 μM) as a function of the concentration of the drug.

and it remains constant (data not shown). Therefore, we can derive the binding parameters accordingly:

$$\phi_1 = \frac{\phi_1^\infty - \phi_1^0}{C} C_B + \phi_1^0 \tag{10}$$

where ϕ_1^0 and ϕ_1^∞ are the rotational correlation times at [HSA]=0 and [HSA]=∞, respectively. C is the total copolymer concentration and C_B is the concentration of bound copolymer that can be related to the thermodynamic parameters of the equilibrium by [39]:

$$C_B = 0.5\left[(nP + C + K_d) - \sqrt{(nP + C + K_d)^2 - 4nPC}\right] \tag{11}$$

In this equation, n is the number of binding sites per HSA protein, P is the total HSA concentration and K_d is the dissociation constant of the [HPMA-copolymer CPT]$_n$:HSA complex in micromolar units. The continuous lines in Fig. 5 are the fitting curves obtained by Eqs. (10) and (11). The fitting parameters ϕ_1^∞, ϕ_1^0 and K_d are shown in Table 1.

4. Discussion

4.1. The shape in solution

CPT interacts considerably with the copolymer, resulting in a heterogeneity of the excited state relax-

ation. This conclusion derives from the analysis of the spectroscopic properties of CPT. The shape of the emission spectrum remains essentially the same, but a two-fold quenching of the fluorescence is found for the drug covalently bound through its α-hydroxyl group to the copolymer (Fig. 1). However, there is no compelling evidence for a wide heterogeneity of binding modes of CPT. In fact, a Lorentzian analysis does not improve the fit of the fluorescence decay as compared to a double-exponential function. Therefore, HPMA-copolymer CPT in isotonic buffered solutions has two discrete lifetimes, which are also far one from the other. The component with the longer lifetime can be ascribed to those CPT molecules deeply buried and shielded from the solvent, while the component with the shorter lifetime could be due to an intra-molecular interaction between CPT molecules that leads to fluorescence quenching.

The spectroscopic behavior of CPT depends on the copolymer concentration. In fact, the average lifetime ($\tau_M=\tau_1 f_1+\tau_2 f_2$) and the normalized fluorescence intensity (F_{436}/C, where C is the concentration) are not constant (Fig. 6). Both τ_M and F_{436}/C increase steadily up to a plateau, which is reached at $\cong 1$ μg/ml,

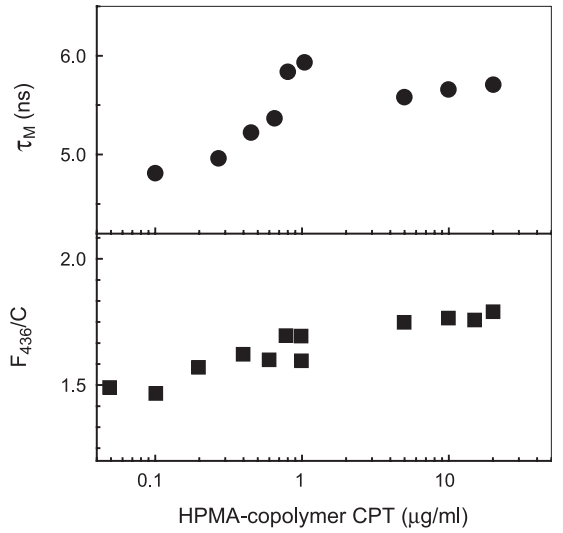

Fig. 6. Average lifetime and normalized intensity of HPMA-copolymer CPT. Upper panel: average lifetime, $\tau_M=\tau_1 f_1+\tau_2 f_2$; lower panel: fluorescence intensity (arbitrary units) at 436 nm normalized to HPMA-copolymer CPT concentration. Error bars are of the same magnitude of the symbol dimension or less.

suggesting either a change in the apparent quantum yield or a redistribution between the two lifetime populations. These changes could be due to different aggregation states of the copolymer as it is also suggested by fluorescence anisotropy (Fig. 3). Therefore, in addition to direct interactions between CPT and HPMA-copolymer, also intermolecular interactions may be responsible for changes in the emission properties of CPT. The drug, which might be partially exposed to the solvent in the unimer (i.e. not aggregated), becomes even more shielded upon aggregation.

The analyses of the relative amplitudes of the two rotational correlation times (Eq. (4)) further support this conclusion. If we assume that a square well potential describes a hindered CPT rotation, the maximum angle spanned by the drug can be obtained from [27,40]:

$$1-g_1=g_2=\left[\frac{\cos\theta(1+\cos\theta)}{2}\right]^2 \qquad (12)$$

The trend of the limit angle θ parallels that of the rotational correlation time ϕ_1 (Fig. 3) and shows that aggregation severely reduces the CPT lateral motion. Our results are in agreement with previous studies [41] in which intra-and intermolecular micelles in aqueous solutions have been observed with other HPMA-copolymers drug conjugates.

The molecular size of the aggregates can be inferred from the combined analysis of the rotational and translational diffusions. The structural data of the HPMA copolymers available from literature (persistence length=3.3–4.0 nm [2,26], average contour length $\sim$35 nm and $R_G\cong 4.3$–4.7 nm [42–45]) indicate that HPMA-CPT copolymers are in a compact conformation under our experimental conditions. Previous analyses of the intrinsic viscosity [26] of similar drug conjugates [46] lead to similar conclusions. However, the overall rotational diffusion of HPMA-CPT copolymer is described by a single rotational correlation time (i.e. the long component, ϕ_1). How this can be related to the structural features? The theory [34] says that the FA of an arbitrary shaped rotor depends upon five correlation times. We have verified by numerical simulations that, when all axial ratios are smaller than 10, data can be well described by a single correlation time [32]. In this case, the difference between the best-fitted rotational correla-

tion time and the harmonic average (Eq. (7)) is within the typical experimental uncertainty of few percents. Only for axial ratios >10 (i.e. more elongated shapes) the difference between rotational correlation times becomes detectable, and the FA decay has to be analyzed by multiple exponential functions. Therefore, our data on HPMA-copolymer CPT suggest that, on the average, the aggregates have an elongated shape with small (<10) axial ratios.

4.2. The aggregation orders

Since we are not able to determine the orientation of CPT moieties with respect to the principal axes of the HPMA-copolymer, we compute the harmonic average, ϕ_{harm}, of the rotational correlation times for a cylinder (Eq. (7)). Computation of the cylinder length and radius is carried out assuming a constant molecular volume, V_2M_n, where V_2=0.9 cm^3/g [47] is the partial molar volume and M_n=25,300 Da is the average molecular weight (19,300 Da) plus one hydration shell. On one hand, for an axial ratio ρ=4, we compute $\phi_{harm} \cong 14.9$ ns, which is in good agreement with the value measured in very dilute solutions (see Table 2). On the other hand, to reproduce the experimental value $\phi_1 \cong 23.0 \pm 1.3$ ns, measured at 0.5 μg/ml, we need to assume an aggregation number of 2, a side-by-side interaction, and an axial ratio ρ between 3 and 4 (Table 2). Polydispersity (1.07) adds a 7% uncertainty on ϕ_{harm} values and, therefore, does not affect our previous conclusions.

Polydispersity and molecular shape affect translational and rotational diffusions in different ways. Also the translational diffusion coefficient can be corrected [48] for polydispersity, as reported in detail in Appendix A. Accordingly, the translational diffusion coefficient is underestimated by 3–4% [43]. The correction raises the average translational diffusion coefficient from 58±4 to 60±4 $\mu m^2/s$ when HPMA-copolymer CPT concentration is below 350 μg/ml (see Fig. 4) and it is negligible for our analysis.

As for the dependence of the translational diffusion on the molecular shape, we have applied computations similar to those used for correcting the rotational diffusion times [31] (Table 2). The simulated values range from 61.9 to 58.8 for side-by-side aggregates of order two and axial ratio between 3 and 4 and well reproduce the experimental values (Table 2). Thus, both rotational and translational diffusions suggest that HPMA-CPT copolymers aggregate below 350 μg/ml in a side-by-side conformation of order 2 in which the unimer has an axial ratio between 3 and 4.

In Fig. 7, we show a direct comparison between translational and rotational diffusions in order to provide a picture of the molecular aggregation in the whole range of the copolymer concentration. The normalized diffusion coefficient ratios in Fig. 7 take into account the different dependence of the translational and rotational diffusions on the molecular size [31,35]. The results of simulations are shown as a dashed area, which accounts for the uncertainty due to 1.07 polydispersity.

The transition from unimer to aggregate of order two, is well detectable by rotational diffusion. Ac-

Table 2
Numerical simulations of rotational and translational diffusion coefficients for HPMA-copolymer CPT unimers and aggregates of association number=2 in comparison with the experimental value

Simulated values					Experimental values		
	Unimer	Aggregation number=2	Aggregation number=2	Axial ratio	Concentration range		
		Side-by-side	Head-to-tail		0–0.5 μg/ml	0.6–1 μg/ml	50–350 μg/ml
ϕ_{harm} (ns)	13.8	22.8	32.5	3	–	–	–
D ($\mu m^2/s$)	68.7	61.9	46.0	3	–	–	–
ϕ_{harm} (ns)	14.9	24.7	33.9	4	–	–	–
D ($\mu m^2/s$)	64.5	58.8	42.4	4	–	–	–
ϕ_1 (ns)	–	–	–	–	14.4±1	23±1.3	–
D ($\mu m^2/s$)	–	–	–	–	–	–	60±4

ϕ_{harm} is the harmonic average of the rotational correlation time obtained from Eq. (7) (see text). The computed translational diffusion coefficient D is obtained from Eq. (9) (Section 2).

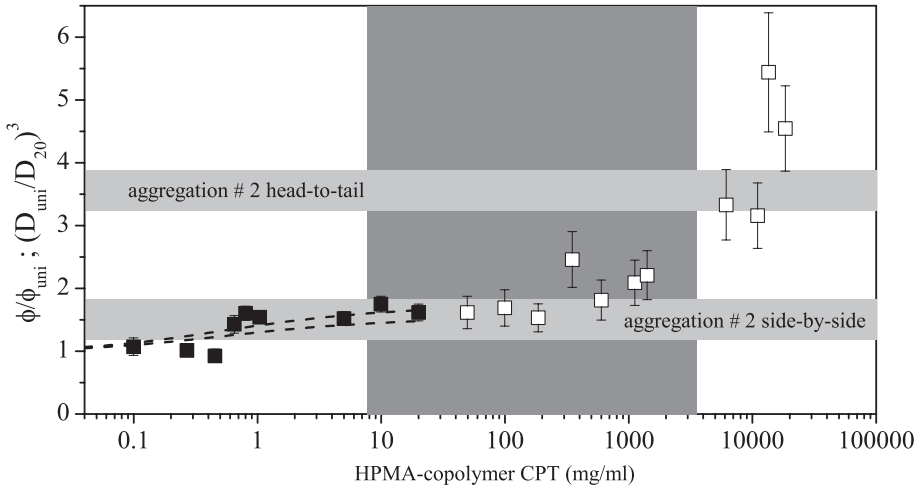

Fig. 7. Normalized diffusion coefficients versus HPMA-copolymer CPT concentration. Normalization is achieved by considering the suitable ratio between experimental and simulated values, ϕ_{uni} and D_{uni}. In both cases, simulated values refer to a unimer with axial ratio ~3.5. Filled squares: rotational diffusion ratio ϕ_1/ϕ_{uni} obtained by fluorescence anisotropy up to 20 μg/ml; ϕ_{uni}=14.35 ns. Open squares: translational diffusion ratio $(D_{uni}/D_{20})^3$ obtained by dynamic light scattering from 0.05 to 20 mg/ml; D_{uni}=66.6 μm^2/s. Light gray areas: distribution of diffusion ratios as predicted for aggregates of order 2, polydispersity 1.07, unimer M_n=19,300 Da (Table 2). The curves describe the best-fitted range from Eq. (13) obtained for the minimum and the maximum values of ϕ_{SS}/ϕ_{uni}=1.55 and ϕ_{SS}/ϕ_{uni}=1.75. In order to take into account the polydispersity of the solution (M_w/M_n=1.07), we add to the values ϕ_{uni}=14.35 ns and D_{uni}=66.6 μm^2/s (Table 2) a 7% uncertainty, while for the aggregate of order n=2 we have added an uncertainty of 10%. The dark gray area outlines the range of concentrations found in plasma of mice treated with a single injection of 220 mg/kg HPMA-copolymer CPT up to 72 h after administration (see Fig. 8).

cordingly, we can estimate an aggregation constant K_a=1.3±0.5 ml/μg from the relationship:

$$\frac{\phi_1}{\phi_{uni}} \cong \frac{\phi_{SS}}{\phi_{uni}} - \left(1 - \frac{\phi_{SS}}{\phi_{uni}}\right) \frac{\left\{1 - \sqrt{1 + 8K_a[C_{copolymer}]}\right\}}{4K_a[C_{copolymer}]} \quad (13)$$

where ϕ_{uni} is the simulated value of the rotational correlation time for the unimer and ϕ_{SS}=23.7±2 ns is the simulated value for a order 2 side-by-side aggregate with axial ratio=3.5. The uncertainty is due to polydispersity.

The translational diffusion indicates that aggregates of order two are stable up to ≅1 mg/ml and that multimeric (n>2) associates form only above this concentration. The copolymer aggregation should be driven by CPT hydrophobic shielding that induce the formation of unimolecular micelles as suggested by Ulbrich et al. [41] and Searle et al. [49] and could promote the aggregation into bimolecular micelles that are stable over four decades. Two indirect evidences of the hydrophobic driven copolymer aggregation, at a concentration very close to 0.5 μg/ml, come from the change of CPT limit angle θ (Fig. 3), whose decrease indicates a lower intra-molecular mobility, and from the increase of the fluorescence lifetime (see Fig. 6). Further aggregation may be possible via unspecific association between copolymers at much higher concentrations, leading to a smooth increase of the diffusion ratio for [HPMA-copolymer CPT]>2 mg/ml as shown in Fig. 7. These observations might be widespread in drug delivery systems in which a small hydrophobic molecule is carried by an hydrophilic copolymer in aqueous solvents. However, similar HPMA copolymers show different aggregation properties depending upon the drug moiety. In particular HPMA-Meso-chlorine e6 [50,51] copolymers shows negligible intermolecular aggregation but relevant intra-molecular interactions, while HPMA-zinc(II) phthalocyanine copolymers [52] display a strong random intermolecular aggregation. The system studied here shows an intermediate

behavior probably due to a balance between the intra-and inter-molecular interactions.

4.3. Binding to serum albumin

As we have recently showed [8], repeated administration of HPMA-copolymer CPT induces relevant tumor growth inhibition in a variety of human tumor xenografts in mice. Activity is observed between 15 and 22.5 mg/kg/day of equivalent CPT, corresponding to a total dose of copolymer from 150 to ~250 mg/kg/day. In mice, the administration of a single dose of 220 mg/kg HPMA-copolymer CPT gave rise to an initial mean plasma concentration of ~3.3 mg/ml, which decreases to ~7 μg/ml after 72 h (Fig. 8). These concentrations are also outlined (gray area) in Fig. 7. From our study, we might infer that aggregates of order 2 could then be present in plasma of treated mice.

Since albumin is by far the major component of plasma and it is very conserved inter-species, we finally investigate the interaction of HPMA-copolymer CPT with HSA in vitro. Binding is measured by titrating solutions at 0.34, 1.7 and 10 μg/ml HPMA-copolymer CPT. The copolymer concentrations are chosen to cover a range from below to well above the K_a^{-1}, which represents the equilibrium between unimer and aggregates of order 2 (see Fig. 7). Eqs. (10) and (11) well describe the titration curves with a 1:1 stoichiometry (n=1) for the copolymer–protein complex. This assumption comes from the plateau values of the global rotational time $\phi \cong 60$ ns, which are reasonably close to the sum $\phi_{HSA}+\phi_{(HPMA\text{-}copolymer\ CPT)}$ where ϕ_{HSA}= 40±2 ns is the known HSA rotational correlation time [53] and $\phi_{(HPMA\text{-}copolymer\ CPT)}$ is the rotational correlation time of the copolymer (≅20 ns in Fig. 7). It is highly unlikely that the 60-ns plateau value for the rotational time is compatible with a binding stoichiometry n=2 unless an unusually compact HSA-(HPMA-CPT copolymer) compound is formed. The dissociation constant depends inversely on the aggregation state of the copolymer, increasing from 1.8±0.4 to 42±6 μM (Table 1). Only at very high dilution, when aggregation is negligible, the copolymer–HSA interaction reproduces that observed for free CPT. Therefore, the interaction with the serum protein may be mainly driven by CPT, the availability of which depends on the aggregation.

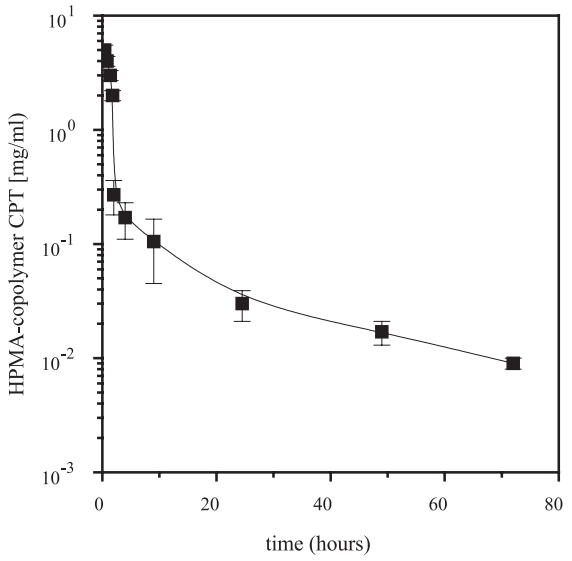

Fig. 8. Mean concentration (out of three independent measurements) of HPMA-copolymer CPT in plasma from mice treated with 220 mg/kg of conjugate. Concentration of HPMA-copolymer CPT was determined in aliquots of plasma collected from 5 min to 72 h after a single intravenous administration and expressed as mg conjugate/ml.

5. Conclusions

We have investigated the aggregation properties of a HPMA-copolymer CPT (at 9.1% CPT content w/w and 1.07 polydispersity), in which the drug is linked through the biodegradable spacer-glycyl-6-aminohexanoyl-glycyl-in a wide range of concentrations from 0.1 μg/ml to 20 mg/ml. These include the plasma levels measured in mice treated with an active dose of the conjugate. We have carried out a meticulous analysis of rotational and translational diffusion of the copolymer by fluorescence spectroscopy and dynamic light scattering, taking into account the effects that polydispersity (low in our case) and shape have on the two types of measurements. This analysis suggests that at physiological conditions in dilute solutions, HPMA-copolymer CPT has an average aggregation number of 2, and that the shape of the aggregates, although elongated, has a low axial ratio between 3 and 4. This aggregation

state remains stable over a wide range of concentrations (up to ~200 μg/ml). Above that, a continuous aggregation process seems to take place. Our data underline the importance of investigating the behavior of polymeric drug carriers in buffer solutions, at conditions as close as possible to physiological ones. They can help interpreting in vivo pharmacokinetic and biological results. We suggest that the circulating species in the plasma of mice treated with biological active doses [8] could be aggregates not higher than order 2, with a reduced affinity for serum albumin. Our results help in giving a microscopic view of the outcome of the first clinical study on HPMA-glycyl-6-aminohexanoyl-glycyl-copolymer CPT [10] (the polydispersity of which was not reported). Schoemaker et al. [10] show that no difference in terminal half-lives or clearance of the copolymer was observed as a function of the dose level, and the administered doses were mainly excreted (68+18%) by the kidneys within 4 days. The plasma levels measured in men at the dose of 68 mg m^{-2} day^{-1} (Fig. 2 of Ref. [10]) seem to be comparable to those measured in our mice experiments (Fig. 8) and therefore they would fall within the gray area of Fig. 7. This suggests that aggregates of order higher than 2 are improbable or present in minor extent also in men, and gives an interpretation at the molecular level of why the circulating species can be excreted by passive filtration in the kidneys [54], while intermolecular interactions are present.

This study advances therefore the interpretation of the pharmacokinetics and toxicity of the conjugate in vivo on the basis of the aggregation and protein binding properties. Future studies are welcome in order to correlate the effect of polydispersity of typical pharmaceutical preparations (1.5–1.7) on drug aggregation and retention.

Acknowledgements

We thank Antonino Suarato and Cristina Geroni, Pharmacia for providing pHPMA-CPT. This work has been partially fund by Italian Ministry of Research (MIUR) as FISR 2003 to V.C. and G.C., and by a fellowship of European Social Fund (FSE-INFM) to F.O.

Appendix A

The Schutz function [48] is used to describe the distribution of masses in a polydispersed solution:

$$P(M,\bar{M},t)=\left(\frac{t+1}{\bar{M}}\right)^{t+1}\frac{M^t}{\Gamma(t+1)}\exp[-M(t+1)/\bar{M}] \tag{14}$$

where $\bar{M}$ is the average mass and t is a parameter related to the width of the distribution as: $(\langle M^2\rangle-\langle M\rangle^2)/\langle M\rangle^2=(t+1)^{-1}$. Γ indicates the incomplete Gamma function and the polydispersity of the distribution is given by: $\langle M^2\rangle/\langle M\rangle^2=1+(t+1)^{-1}$. The computation of the average translational diffusion coefficient can be made by assuming a dependence of the diffusion coefficient on the molecular mass, $D(M)=d_0M^{\varepsilon}$, where ε is a fractional exponent and d_0 is a constant depending on the temperature and the viscosity of the solution [43]. The average diffusion coefficient can be obtained from the ratio of two moments of the Schutz function:

$$\frac{\langle D_T\rangle}{d_0}=\frac{\langle M^{2+\alpha}\rangle}{\langle M^2\rangle}=\frac{\int_0^\infty \mathrm{d}MP(M)M^{2+\alpha}}{\int_0^\infty \mathrm{d}MP(M)M^2} \tag{15}$$

The moments of the Schutz distribution are:

$$\langle M^\beta\rangle=\frac{\bar{M}^\beta}{(t+1)^\beta}\frac{\Gamma(t+1+\beta)}{\Gamma(t+1)} \tag{16}$$

If we assume a dependence of the diffusion coefficient on the inverse of the third power of the mass, $\varepsilon=1/3$ and the average translational diffusion coefficient is given by:

$$\langle D_T\rangle=d_0\frac{(t+1)^{1/3}}{\bar{M}^{1/3}}\frac{\Gamma(t+8/3)}{\Gamma(t+3)} \tag{17}$$

The correction factor for $t=0.428$, which corresponds to a polydispersity $\langle M^2\rangle/\langle M\rangle^2=1.07$, is $(t+1)^{1/3}\Gamma(t+8/3)/\Gamma(t+3)\cong 0.97$ indicating that the measured diffusion coefficients must be raised by ≅3%. When assuming $\varepsilon=1/2$, we estimate a correction of ≅4%.

References

[1] A.K. Patri, I.J. Majoros, J.R. Baker Jr., Dendritic polymer macromolecular carriers for drug delivery, Curr. Opin. Chem. Biol. 6 (2002) 466–471.

[2] R. Langer, Drug delivery and targeting, Nature 392 (1998) 5–10 (suppl.).

[3] R. Langer, Selected advances in drug delivery and tissue engineering, J. Control. Release 62 (1999) 7–11.

[4] J. Kopecek, P. Kopeckova, T. Minko, Z. Lu, HPMA copolymeranticancer drug conjugates: design, activity, and mechanism of action, Eur. J. Pharm. Biopharm. 50 (2000) 61–81.

[5] H. Maeda, L.M. Seymour, Y. Miyamoto, Conjugates of anticancer agents and polymers: advantages of macromolecular therapeutics in vivo, Bioconjug. Chem. 3 (1992) 51–362.

[6] R.E. Perdue, R.L. Smith, M.E. Wall, J.L. Hartwell, B.J. Abbott, Camptotheca acuminata decaisne (nyssaceae), source of camptothecin, an antileukemic alkaloid, Technical Bulletin, vol. 1415, U.S. Department of Agriculture, Agricultural Research Service, Washington, DC, 1970.

[7] J.A. Gottlieb, A.M. Guarino, J.B. Call, V.T. Oliverio, J.B. Block, Preliminary pharmacologic and clinical evaluation of camptothecin sodium (NSC-100880), Cancer Chemother. Rep., Part 1 54 (1970) 461–470.

[8] M. Zamai, M. VandeVen, M. Farao, E. Gratton, A. Ghiglieri, M.G. Castelli, E. Fontana, R. D'Argy, A. Fiorino, E. Pesenti, A. Suarato, V.R. Caiolfa, Camptothecin, poly[*n*-(2-hydroxypropyl) methacrylamide] copolymers in antitopoisomerase-I tumor therapy: intratumor release and antitumor efficacy, Mol. Cancer Ther. 2 (2003) 29–40.

[9] F.M. Muggia, P.-J. Creaven, H.H. Hansen, M.H. Cohen, O.S. Sealwry, Phase I clinical trial of weekly and daily treatment with camptothecin (NSC-100880): correlation with preclinical studies, Cancer Chemother. Rep. 56 (1972) 515–521.

[10] N.E. Schoemaker, C. van Kesteren, H. Rosing, S. Jansen, M. Swart, J. Lieverst, D. Fraier, M. Breda, C. Pellizzoni, R. Porro, M.G. Porro, J.H. Beijnen, J.H.M. Scellens, W.W. ten Bokkel Huinink, A phase I and pharmacokinetic study of MAG-CPT, a water-soluble polymer conjugate of camptothecin, Br. J. Cancer 87 (2002) 608–614.

[11] C.G. Moertel, A.J. Schutt, R.J. Reitemeier, R.G. Hahn, Phase II study of camptothecin (NSC-100880) in the treatment of advanced gastrointestinal cancer, Cancer Chemother. Rep. 56 (1972) 95–101.

[12] J.A. Gottlieb, J.K. Luce, Treatment of malignant melanoma with camptothecin (NSC-100880), Cancer Chemother. Rep. 56 (1972) 103–105.

[13] Y.H. Hsiang, R. Hertzberg, S. Hecht, L.F. Liu, Camptothecin induces protein-linked DNA breaks via mammalian DNA topoisomerase, Int. J. Biol. Chem. 26 (1985) 14873–14878.

[14] Y.H. Hsiang, L.F. Liu, M.E. Wall, M.C. Wani, A.W. Nicholas, G. Manikumar, S. Kirschenbaum, R. Silber, M. Potmesil, DNA topoisomerase I-mediated DNA cleavage and cytotoxicity of camptothecin analogues, Cancer Res. 4 (1989) 4385–4389.

[15] K.W. Kohn, Y. Pommier, Molecular and biological determinants of the cytotoxic actions of camptothecins. Perspective for the development of new topoisomerase I inhibitors, Ann. N. Y. Acad. Sci. 92 (2000) 11–26.

[16] B.C. Giovanella, J.S. Stehlin, M.E. Wall, M.C. Wani, A.W. Nicholas, L.F. Liu, R. Silber, M. Potmesil, DNA topoisomerase I-targeted chemotherapy of human colon cancer in xenografts, Science 246 (1989) 1046–1048.

[17] M. Potmesil, Y.H. Hsiang, L.F. Liu, B. Bank, H. Grossberg, S. Kirschenbaum, T.J. Forlenza, A. Penziner, D. Kanganis, T.J. Forlenzar, Resistance of human leukemic and normal lymphocytes to drug-induced DNA cleavage and low levels of DNA topoisomerase II, Cancer Res. 48 (1988) 3537–3543.

[18] L.L. Jung, W.C. Zamboni, Cellular, pharmacokinetic, and pharmacodynamic aspects of response to camptothecins: can we improve it? Drug Resist. Updat. 4 (2001) 273–288.

[19] V.R. Caiolfa, M. Zamai, A. Fiorino, E. Frigerio, C. Pellizzoni, R. d'Argy, A. Ghiglieri, M.G. Castelli, M. Farao, E. Pesenti, M. Gigli, F. Angelucci, A. Suarato, Polymer-bound camptothecin: initial biodistribution and antitumour activity studies, J. Control. Release 65 (2000) 105–119.

[20] R. Duncan, Polymer-drug conjugates: potential for improved chemotherapy, Anti-Cancer Drugs 3 (1992) 175–210.

[21] L.J. Nugent, R.K. Jain, Extravascular diffusion in normal and neoplastic tissues, Cancer Res. 44 (1984) 38–244.

[22] F. Yuan, M. Dellian, D. Fukumura, M. Leunig, D.A. Berk, V.P. Torchilin, R.K. Jain, Vascular permeability in a human tumor xenograft: molecular size dependence and cutoff size, Cancer Res. 55 (1995) 3552–3756.

[23] H. Maeda, in: A.J. Domb (Ed.), Polymeric Site-Specific Pharmacotherapy, Wiley, New York, 1994, pp. 95–116.

[24] L.W. Seymour, K. Ulbrich, P.S. Steyger, M. Brereton, V. Subr, J. Strohalm, R. Duncan, Tumouri tropism and anticancer efficacy of polymer-based doxorubicin prodrugs in the treatment of subcutaneous murine B16F19 melanoma, Br. J. Cancer 70 (1994) 636–641.

[25] R. Duncan, H.C. Cable, J.B. Lloyd, P. Rejmanova, J. Kopecek, Degradation of side-chains of *N*-(2-hydroxyproply)methacrylamide co-polymers by lysosomal thiol-proteinases, Biosci. Rep. 2 (1983) 1041–1046.

[26] R. Mendichi, V. Rizzo, M. Gigli, G. Razzano, F. Angelucci, metti Schieroni, A. Giacometti Schieroni, Molar mass distribution of a polymer-drug conjugate containing the antitumour drug paclitaxel by size exclusion chromatography and universal calibration, J. Liq. Chromatogr. Relat. Technol. 21 (1998) 129–139.

[27] J.R. Lakowicz, Principles in Fluorescence Spectroscopy, Plenum, New York, 1983.

[28] R.B. Thompson, E. Gratton, Phase fluorometric method for determination of standard lifetimes, Anal. Chem. 60 (1988) 670–674.

[29] J.R. Lakowicz, G. Laczko, H. Cherek, E. Gratton, M. Linkeman, Analysis of fluorescence decay kinetics from variable-frequency phase shift and modulation data, Biophys. J. 46 (1984) 463–477.

[30] M. Collini, G. Chirico, G. Baldini, DNA torsional dynamics by multifrequency phase fluorometry, Biopolymers 32 (1992) 1447–1459.

[31] M.M. Tirado, J. Garcia de la Torre, Rotational dynamics of

rigid, symmetric top macromolecules. Application to circular cylinders, J. Chem. Phys. 73 (4) (1980) 1986–1993.
[32] R.F. Steiner, Anisotropy: theory and application, in: J.R. Lakowicz (Ed.), Topics in Fluorescence Spectroscopy, vol. 2, Plenum, New York, 1991, pp. 1–52.
[33] G. Chirico, M. Gardella, Photon correlation spectroscopy to 10 ns resolution, Appl. Opt. 38 (1999) 2059–2067.
[34] B.J. Berne, R. Pecora, Dynamic Light Scattering, Wiley, New York, 1975.
[35] M.M. Tirado, J. Garcia de la Torre, Translational friction coefficients of rigid, symmetric top macromolecules. Application to circular cylinders, J. Chem. Phys. 71 (6) (1979) 2581–2587.
[36] K.S. Schmitz, An introduction to DLS by macromolecules, Academic Press, Boston, 1990, p. 56 and p. 106.
[37] M. Corti, V. Degiorgio, Quasi-elastic light scattering study of intermicellar interactions in aqueous sodium dodecyl sulfate solutions, J Phys. Chem. 85 (1981) 711–717.
[38] S. Beretta, G. Chirico, D. Arosio, G. Baldini, Photon correlation spectroscopy of interacting and dissociating hemoglobin, J. Chem. Phys. 106 (1997) 8427–8435.
[39] C.R. Cantor, P.R. Schimmel, Biophysical Chemistry: Part III. The Behavior of Biological Macromolecules, Freeman, San Francisco, 1980.
[40] G. Lipari, A. Szabo, Effect of librational motion on fluorescence depolarization and nuclear magnetic resonance relaxation in macromolecules and membranes, Biophys. J. 30 (1980) 489–506.
[41] K. Ulbrich, Č. Koňák, Z. Tuzar, J. Kopeček, Solution properties of drug carriers based on poly[*N*-(2-hydroxypropyl)methacrylamide] containing biodegradable bonds, Makromol. Chem. 188 (1987) 1261–1272.
[42] R. Mendichi, V. Rizzo, M. Gigli, A. Giacometti-Schieroni, Dilute-solution properties of a polymeric antitumor drug carrier by size exclusion chromatography, viscometry and light scattering, J. Appl. Polym. Sci. 70 (1998) 329–338.
[43] M. Doi, S.F. Edwards, The Theory of Polymer Dynamics, Clarendon Press, Oxford, 1986, pp. 316–318.
[44] P.J. Flory, Principles of Polymer Chemistry, Cornell Univ. Press, Ithaca, NY, 1953, pp. 428–430.
[45] G. Beaucage, S. Rane, S. Sukumaran, M.M. Satkowski, L.A. Schechtman, Y. Doi, Persistence length of isotactic poly(hydroxy butyrate), Macromolecules 30 (1997) 4158–4162.
[46] R. Mendichi, V. Rizzo, M. Gigli, Fractionation and characterization of a conjugate between a polymeric drug-carrier and the antitumor drug camptothecin, Bioconjug. Chem. 13 (2002) 1253–1258.
[47] J. Brandrup, E.H. Immergut, E.A. Grulke, Polymer Handbook, IV Ed., Wiley-Interscience, Toronto, 1999.
[48] G. Nagaele, On the dynamics and structure of charge stabilized suspensions, Phys. Rep. 272 (1996) 215–372.
[49] F. Searle, S. Gac-Breton, R. Keane, S. Dimitrijevic, S. Brocchini, E.A. Sausville, R. Duncan, *N*-(2-Hydroxypropyl)-methacrylamide copolymer-6-(3-aminopropyl)-ellipticine conjugates. Synthesis, in vitro, and preliminary in vivo evaluation, Bioconjug. Chem. 12 (5) (2001) 711–718.
[50] J.-G. Shiah, C. Konák, J.D. Spikes, J. Kopecek, Influence of pH on aggregation and photoproperties of *N*-(2-hydroxypropyl)methacrylamide copolymer-meso-chlorin e6 conjugates, J. Phys. Chem., B 101 (1997) 119–126.
[51] J.-G. Shiah, C. Konák, J.D. Spikes, J. Kopecek, Solution and photoproperties of *N*-(2-hydroxypropyl)methacrylamide copolymer-meso-chlorin e6, Conjug. Drug Deliv. 5 (1998) 6803–6809.
[52] Z.-W. Gu, V. Omelyanenko, P. Kopeckova, J. Kopecek, C. Konak, Association of a substituted zinc(II) phthalocyanine-*N*-(2-hydroxypropyl)methacrylamide copolymer conjugate, Macromolecules 28 (1995) 8375–8380.
[53] M.L. Ferrer, R. Duchowicz, B. Carrasco, J. Garcia de la Torre, A.U. Acuna, The conformation of serum albumin in solution: a combined phosphorescence depolarization-hydrodynamic modeling study, Biophys. J. 80 (2001) 2422–2430.
[54] K. Blouch, W.M. Deen, J.P. Fauvel, J. Bialek, G. Derby, B.D. Myers, Molecular configuration and glomerular size selectivity in healthy and nephrotic humans, Am. J. Phys. VVVV (1997) 430–437.
[55] P. Bevington, D.K. Robinson, Data Reduction and Error Analysis for the Physical Sciences, McGraw-Hill, New York, 1969, pp. 204–206.